Synthesis and Coordinating Ability of an Anionic Cobaltabisdicarbollide Ligand Geometrically Analogous to BINAP

Isabel Rojo,[a] Francesc Teixidor,[a] Clara Viñas,*[a] Raikko Kivekäs,[b] and Reijo Sillanpää[c]

Abstract: The anionic chelating ligand $[1,1'\text{-}(PPh_2)_2\text{-}3,3'\text{-}Co(1,2\text{-}C_2B_9H_{10})_2]^-$ has been synthesized from $[3,3'\text{-}Co(1,2\text{-}C_2B_9H_{11})_2]^-$ in very good yield in a one-pot process with an easy work-up procedure. The coordinating ability of this ligand has been studied with Group 11 metal ions (Ag, Au) and with transition-metal ions (Pd, Rh). The two dicarbollide halves of the $[1,1'\text{-}(PPh_2)_2\text{-}3,3'\text{-}Co(1,2\text{-}C_2B_9H_{10})_2]^-$ ligand can swing about one axis in a manner analogous to the constituent parts of BINAP and ferrocenyl phosphine derivatives. All these ligands function as hinges, with the most important property in relation to the coordination requirements of the metal being the P···P distance. $[1,1'\text{-}(PPh_2)_2\text{-}3,3'\text{-}Co(1,2\text{-}C_2B_9H_{10})_2]^-$, BINAP, ferrocenyl phosphine derivatives, and other hinge ligands present a range of different P···P separations, and consequently different coordination spheres and dispositions around metal cations. To account for these differences, the equation $D_\varphi^2 = D_0^2 + 4R^2\cos^2(90-\frac{\varphi}{2})$ has been developed. It relates the P···P distance (D_φ) in a complex with the minimum P···P distance (D_0) that is characteristic of the hinge-type ligand.

Keywords: atropisomerism · boranes · homogeneous catalysis · metallacarborane anions · phosphane ligands

Introduction

Today, synthesizing enantiomerically pure compounds is a very significant endeavor in the development of pharmaceuticals, agrochemicals, essences, and flavors.[1] Enantioselectivity can be achieved with both C_1- and C_2-symmetric ligands, utilizing chirality at carbon, chirality on a donor atom (e.g., phosphorus), axial chirality, or planar chirality. In 1968, the groups of Knowles[2] and Horner[3] independently reported the first homogeneously catalyzed hydrogenation of alkenes with chiral monodentate tertiary phosphine–Rh complexes (C_1-symmetric ligands). Later, Kagan and Dang[4] devised DIOP, a C_2-symmetric ligand that represented a major breakthrough in the area. In 1980, Noyori and coworkers published the synthesis of BINAP[5] (2,2′-bis(diphenylphosphanyl)-1,1′-binaphthyl), which is an axially dissymmetric C_2 ligand capable of exerting strong steric and electronic influences on transition-metal complexes. It has found extensive application in asymmetric catalysis.[6] Since then, thousands of chiral ligands and their transition-metal complexes have been reported,[7] and many of them are known to be highly effective in the asymmetric formation of C–H, C–C, C–O, and C–N bonds. A large proportion of them closely resemble BINAP and are obtained in racemic form for subsequent resolution to produce the enantiomeric atropisomers. An example of such a ligand is MeO-BIPHEP, which is depicted along with BINAP and $[1,1'\text{-}(PPh_2)_2\text{-}3,3'\text{-}Co(1,2\text{-}C_2B_9H_{10})_2]^-$, **2**$^-$, in Figure 1. While chiral atropisomeric biaryl diphosphines such as BINAP, BIPHEP, and MeO-BIPHEP are very effective ligands for many asymmetric reactions,[8,9] sometimes they are not efficient for certain substrates due to insufficient rigidity. Introducing a bridge of variable length to link the diaryl groups has been proposed[10] as a means of making rigid ligands with tunable bite angles.[11] Ferrocenyl phosphine ligands (Figure 1) have also been devised.[12] Chiral ligands are produced from the latter by introducing a single substituent.

We had a number of reasons for wishing to prepare metallacarboranyl diphosphines: 1) the rapidly developing field of the chemistry of cobaltabisdicarbollide derivatives provides

[a] Dr. I. Rojo, Prof. F. Teixidor, Dr. C. Viñas
Institut de Ciència de Materials de Barcelona (C.S.I.C.)
Campus de la U.A.B.
08193 Bellaterra (Spain)
Fax: (+34) 935-805-729
E-mail: clara@icmab.es

[b] Dr. R. Kivekäs
Department of Chemistry
P.O. Box 55, University of Helsinki
00014 Helsinki (Finland)

[c] Prof. R. Sillanpää
Department of Chemistry
University of Jyväskylä
40351 Jyväskylä (Finland)

  DOI: 10.1002/chem.200400361

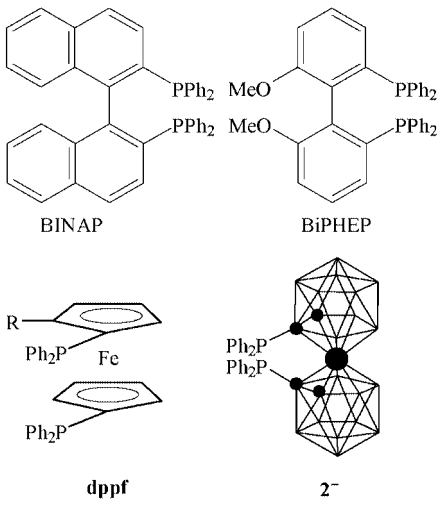

Figure 1. Representations of BINAP, MeO-BIPHEP, a diphenylphosphino ferrocene (dppf), and $[1,1'\text{-}(PPh_2)_2\text{-}3,3'\text{-}Co(1,2\text{-}C_2B_9H_{10})_2]^-$ ($\mathbf{2}^-$).

a pool of unprecedented backbones that may be used to stabilize and/or elaborate any chosen metal centre;[13] 2) to prove that although metallaboranes may look esoteric their stability, color, and reactivity merit their further consideration; 3) to provide novel intrinsically anionic diphosphines as an alternative to sulfonated BINAP,[14] for instance; and finally 4) to show how the metal orientation with respect to the axis of swing can be modulated.

Our aim in presenting this work is to highlight the possibilities of these ligands, derivatives of $[3,3'\text{-}Co(1,2\text{-}C_2B_9H_{11})_2]^-$, $\mathbf{1}^-$, their versatility, and their coordinating abilities. We have not attempted to separate the racemic mixture.

Results

Synthesis of $[1,1'\text{-}(PPh_2)_2\text{-}3,3'\text{-}Co(1,2\text{-}C_2B_9H_{10})_2]^-$, $\mathbf{2}^-$

The desired anionic diphosphine may be conveniently prepared by metalation of $[3,3'\text{-}Co(1,2\text{-}C_2B_9H_{11})_2]^-$ with *n*BuLi, followed by simple reaction with chlorodiphenylphosphine in 1,2-dimethoxyethane (DME). A red solid corresponding to Li-**2** spontaneously separates from the solution, which can then be filtered in air. The NMe_4 or Cs salts of $\mathbf{2}^-$ can be produced by dissolving Li-**2** in ethanol and adding an aqueous solution of $[NMe_4]Cl$ or CsCl. Solids corresponding to the M-**2** (M = NMe_4 or Cs) stoichiometry separate well and can be collected by filtration. The formula of $\mathbf{2}^-$ was established from the mass spectrum obtained by the matrix-assisted laser desorption ionization (MALDI-TOF) technique in the negative-ion mode without the use of a matrix. The absence of a matrix aids the interpretation of the primary and secondary mechanisms. The "primary" mechanism can be regarded as the separation of the anionic cobaltabisdicarbollide derivative from the bonded lithium cation. The "secondary" mechanism can provide some clues about the substituents directly bonded to the cluster carbon atoms. Figure 2 shows the MALDI-TOF mass spectrum of the anion $\mathbf{2}^-$. Peaks corresponding to masses lower than the molecular ion peak at *m*/*z* 691.43 are observed at *m*/*z* 507.33 ($M-PPh_2$) and 323.32 ($M-2\,PPh_2$). Full agreement between the experimental and calculated patterns was obtained for the molecular ion peak. The ^{11}B, ^{1}H, and ^{31}P NMR spectra of $[NMe_4]$-**2** and Cs-**2** were found to be in accord with the proposed structure shown in Figure 1. The $^{11}B\{^1H\}$ NMR spectrum of Li-**2** displays a 1:1:2:2:1:1:1 pattern in the range $\delta = +9.1$ to -20.0 ppm, indicative of a *closo* species with all boron atoms in nonequivalent vertices. The resonances of relative intensity 2 may be attributed to the coincidental overlap of two absorptions of relative intensity 1. This pattern is consistent with single substitution at a cluster carbon

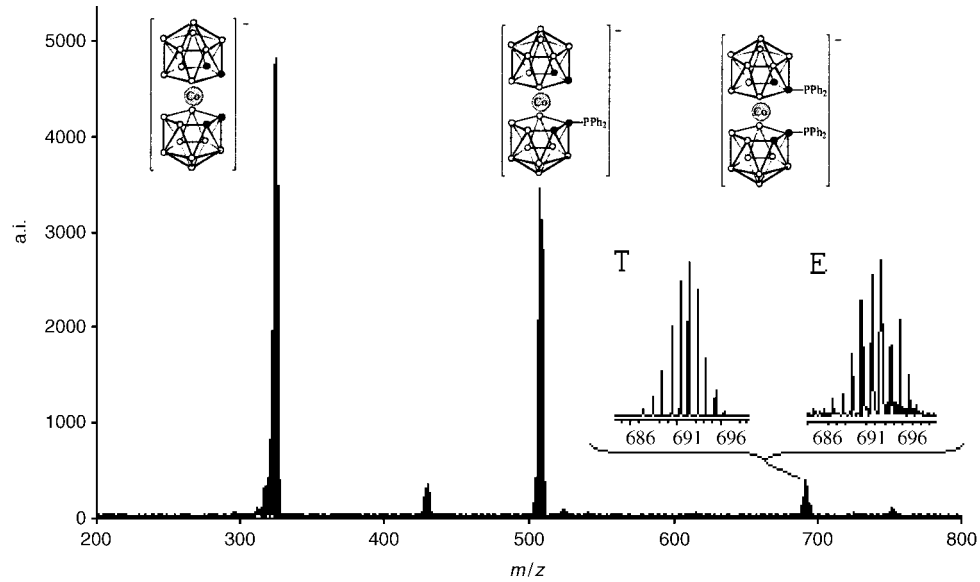

Figure 2. MALDI-TOF mass spectrum obtained for the anionic compound $\mathbf{2}^-$ (T = calculated, E = experimental).

in each dicarbollide moiety. In agreement with this, the $^{31}P\{^1H\}$ NMR spectrum shows only one resonance at δ = 23.48 ppm. Finally, the ^1H NMR spectrum displays a group of resonances between δ = 7.76 and 7.31 ppm corresponding to the aromatic protons and one resonance at δ = 4.37 ppm corresponding to the C_c–H proton (C_c = cluster carbon atom) in a ratio of 20:2. The absence of other peaks in the very informative region of δ = 4.0–4.8 ppm indicates that only one of the three possible geometrical isomers had been generated. These three geometrical isomers (Figure 3) might conceivably have been produced in the reaction, and would have given rise to distinct resonances in the $^{31}P\{^1H\}$ NMR spectrum and similar ^{11}B NMR patterns according to the expected C_2 or C_s symmetries, respectively. Therefore, a crystal structure determination would have been necessary to elucidate which one of the three possible isomers had been generated. However, the $^{13}C\{^1H\}$ NMR spectrum of Li-**2** in the C_c–R (R = H, P) region already provided a good indication of which isomer had been produced. An expanded portion of the $^{13}C\{^1H\}$ NMR spectrum is shown in Figure 4. The spectrum shows one resonance at δ = 61.41 ppm with ^1J(C,P) = 81 Hz and a doublet of doublets centered at δ = 60.22 ppm with ^2J(C,P) = 47 Hz and ^3J(C,P) = 14 Hz. Interestingly, the two observed resonances, C_c–P and C_c–H, do not show the same splitting pattern with phosphorus. The diagrams in Figure 5 offer an explanation for the different splittings of the two C_c atoms. J(C,P) denotes the C coupling with the P in the same dicarbollide moiety, while J'(C,P) denotes the C coupling with P in the other dicarbollide moiety. Figure 5a and Figure 5b correspond to the racemic mixture, while Figure 5c and Figure 5d correspond to the *pseudo-meso* isomer. Figure 5b and Figure 5c refer to the ^{13}C resonance for C_c–P, while Figure 5a and Figure 5d refer to the ^{13}C resonance of C_c–H. The ratio of J(C,P) to J'(C,P), represented by the lengths of the arrows in the figure, is similar in c) and d), and therefore similar splitting patterns would be expected for C_c–P and C_c–H in the *pseudo-meso* form. The J(C,P) versus J'(C,P) discrepancy is very accentuated in the racemic mixture (Figure 5a and Figure 5b), with C_c–H having more similar J and J' values and thus being subjected to greater splitting. This would rationalize the observed pattern in the $^{13}C\{^1H\}$ NMR spectrum of **2**$^-$ and led us to postulate that the racemic isomer had been generated. An X-ray diffraction study of [NMe_4]-**2** confirmed the stereochemistry deduced from the spectroscopic data and revealed that the synthesized geometrical isomer was indeed the racemic form.

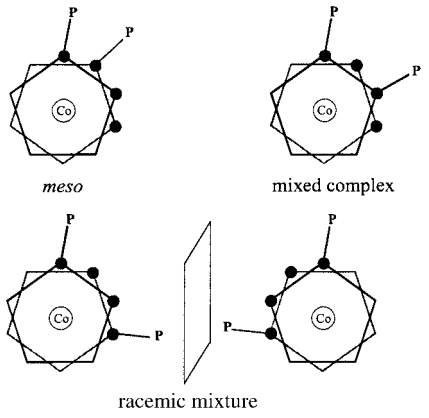

Figure 3. Geometrical isomers of the anionic compound **2**$^-$ (view from the top of the pentagonal faces): a) *pseudo-meso* isomer, b) mixed complex, c) racemic mixture.

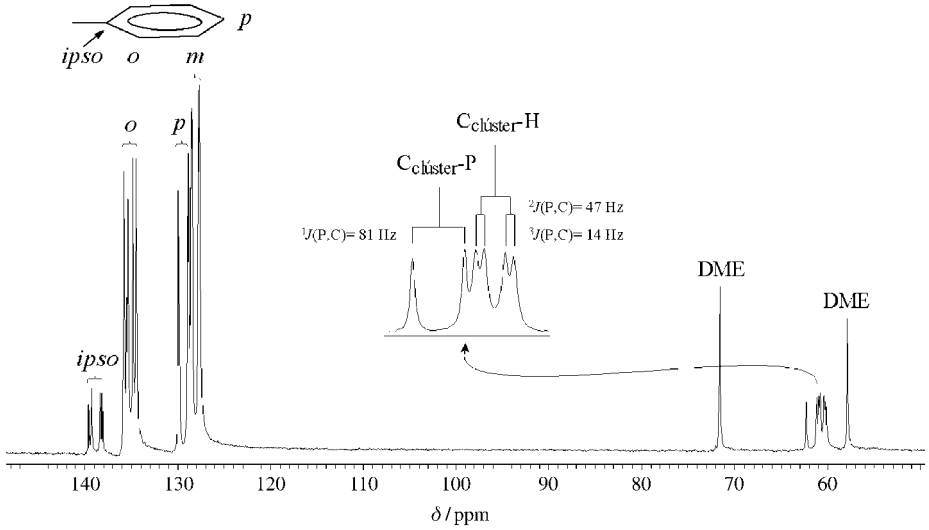

Figure 4. $^{13}C\{^1H\}$ NMR spectrum of **2**$^-$ with a more detailed view of the C_c–R (R = H or P) region.

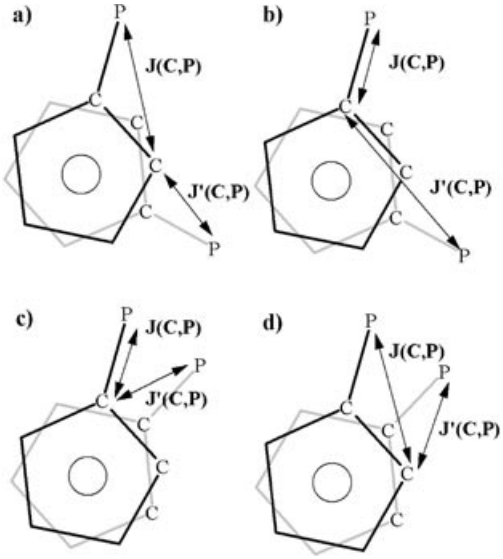

Figure 5. Projection of the pentagonal faces in **2**$^-$ (with cobalt at the center of symmetry): a) and b) correspond to the racemic mixture, while c) and d) correspond to the *meso* isomer.

Crystal structure of [NMe$_4$]-2: Crystals of [NMe$_4$]-**2** suitable for an X-ray diffraction study were obtained by slow evaporation of the solvent from a solution of the compound in acetone. The structure consists of well-separated [NMe$_4$]$^+$ ions and bisdiphenylphosphine cobaltabisdicarbollide **2**$^-$ ions. Figure 6 shows a drawing of the anion; Table 1 lists crystallographic data and Table 2 selected interatomic distances and angles. As expected, the metal in **2**$^-$ is sandwiched by the pentagonal faces of the two dicarbollide units. The pentagonal faces have a mutually staggered conformation, with the torsion angle C1-*c*-*c*′-C1′ being −102.3° (*c* = centroid of C1,C2,B7,B8,B4 face; *c*′ = centroid of C1′,C2′,B7′,B8′,B4′ face), and the P1···P2 distance is 5.1834(19) Å. Thus, the C–PPh$_2$ moieties have a cisoid disposition, showing that the anion corresponds to one of the enantiomers of the racemic form. The symmetry of **2**$^-$ is C_1 in the solid state as the mutual orientations of the PPh$_2$ groups are different.

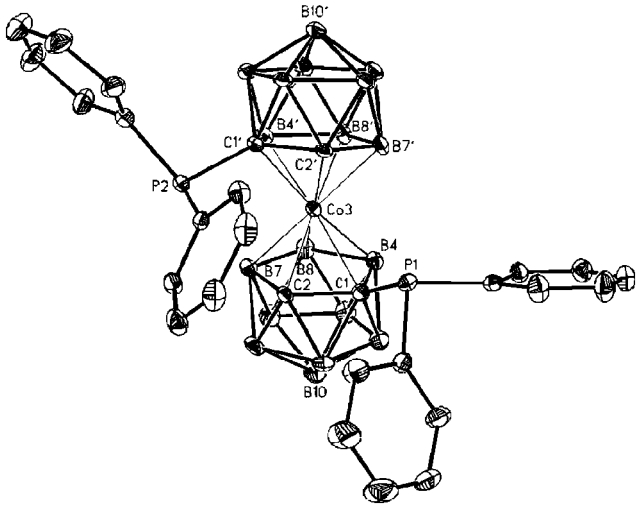

Figure 6. Drawing of the anion of [NMe$_4$]-**2** with 20% thermal displacement ellipsoids.

Table 1. Crystallographic data and structural refinement details for compounds [NMe$_4$]-**2**, **3**·OCMe$_2$, **4**, and **5**.

	[NMe$_4$]-**2**	[**3**·OCMe$_2$]·OCMe$_2$	**4**	**5**
empirical formula	$C_{32}H_{52}B_{18}CoNP_2$	$C_{52}H_{67}AgB_{18}CoO_2P_3$	$C_{46}H_{55}AuB_{18}CoP_3$	$C_{31}H_{46}AgB_{18}CoOP_2$
formula weight	766.20	1178.35	1151.29	858.00
crystal system	monoclinic	monoclinic	monoclinic	monoclinic
space group	$P2_1/n$ (no. 14)	$C2/c$	$P2_1/n$ (no. 14)	$P2_1/n$ (no. 14)
a [Å]	12.705(2)	39.7263(5)	11.15040(10)	12.8241(2)
b [Å]	12.1215(18)	12.5412(2)	18.2288(2)	19.1948(5)
c [Å]	27.988(7)	23.5531(3)	24.9604(2)	16.9761(4)
β [°]	101.416(16)	95.3792(10)	97.0350(10)	108.1789(14)
V [Å^3]	4225.0(14)	11682.8(3)	5035.22(8)	3970.19(15)
Z	4	8	4	4
T [°C]	21	−100	−100	−100
λ [Å]	0.71069	0.71073	0.71073	0.71073
ρ [g cm^{-3}]	1.205	1.340	1.519	1.435
μ [cm^{-1}]	5.08	7.41	33.70	10.20
goodness-of-fit	0.996	1.010	1.015	1.034
$R1$[a] [$I > 2\sigma(I)$]	0.0603	0.0434	0.0253	0.0313
$wR2$[b] [$I > 2\sigma(I)$]	0.1379	0.0867	0.0488	0.0672

[a] $R1 = \Sigma||F_o|-|F_c||/\Sigma|F_o|$. [b] $wR2 = \{\Sigma[w(F_o^2-F_c^2)^2]/\Sigma[w(F_o^2)^2]\}^{1/2}$.

Table 2. Selected interatomic distances [Å] and angles [°] for [NMe$_4$]-**2**.

Co3–C1	2.157(5)	Co3–C2	2.072(4)	Co3–B8	2.116(6)
Co3–C1′	2.147(4)	Co3–C2′	2.094(4)	Co3–B8′	2.122(6)
P1–C1	1.896(5)	P2–C1′	1.893(4)	C1–C2	1.650(6)
C1′–C2′	1.612(6)				
C1′-Co3-C1	135.07(17)	P1-C1-Co3	108.3(2)	C2-C1-P1	114.4(3)
B4-C1-P1	128.2(3)	P2-C1′-Co3	111.3(2)	C2′-C1′-P2	122.9(3)
B4′-C1′-P2	120.8(3)	B10-Co3-B10′	173.84(14)		

Coordinating ability

Two types of metal ions were studied to assess the coordinating ability of **2**$^-$. First, Group 11 elements (Ag, Au) were studied in view of their tendency to offer lower coordination numbers than other transition-metal ions, which would provide information on the real chelating predisposition of **2**$^-$; second, transition-metal ions of well-recognized catalytic importance (Pd, Rh) were studied.

With Group 11 elements (Ag, Au): Treatment of [NMe$_4$]-**2** with one equivalent of [MCl(PPh$_3$)] (M = Ag, Au) for 0.5 h in refluxing ethanol afforded complexes [M(**2**)(PPh$_3$)] (M = Ag, **3**; Au, **4**) in 71 and 98% yield, respectively. Similarly, treatment of [NMe$_4$]-**2** with one equivalent of AgClO$_4$ at room temperature overnight in ethanol/acetone (10:3) afforded [Ag(**2**)(OCMe$_2$)] (**5**) in 88% yield (Figure 7).

The molecular structure of **4** in solution was deduced from its $^{31}P\{^1H\}$ and $^{11}B\{^1H\}$ NMR spectra in [D$_6$]acetone. Interestingly, the spectra were more readily acquired at −60 °C than at room temperature. The $^{11}B\{^1H\}$ NMR spectrum displayed a 1:1:2:2:1:1:1 pattern, in agreement with C_2 symmetry, in the range $\delta = +10.0$ to −19.4 ppm. The $^{31}P\{^1H\}$ NMR spectrum was found to be simple, showing two sets of resonances: a doublet at δ = 73.61 ppm with ^2J(P,P) = 146 Hz and a triplet at δ = 45.06 ppm with the same *J* value. This is in full agreement with the Au being trigonally coordinated, as shown in Figure 7.

The structural elucidation and behaviour of **3** in solution proved to be more complex. In principle, a molecular structure such as that found for **4** would be expected, in accord with the molecular structure of [Ag{7,8-(PPh$_2$)$_2$-7,8-C$_2$B$_9$H$_{10}$}(PPh$_3$)],[15] in which the chelating anionic *nido* carboranyl diphosphine ligand has the two phosphorus atoms in adjacent positions in the same dicarbollide moiety. The $^{31}P\{^1H\}$ NMR spectrum of **3** was also more readily acquired

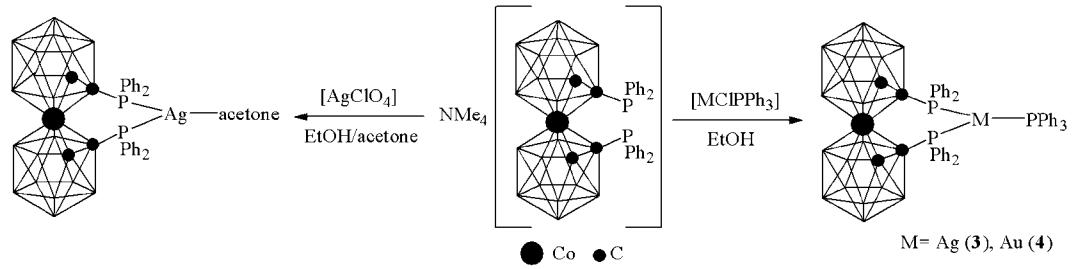

Figure 7. Scheme summarizing the reactions of $[NMe_4]$-**2** with $[MClPPh_3]$ (M = Ag, Au) and with $[AgClO_4]$; non-specified vertices are BH.

at −60 °C than at room temperature, and was again relatively simple with two absorptions at $\delta = 43.50$ and 42.81 ppm, and a third one at $\delta = 32.89$ ppm. Each absorption in fact comprises two doublets as a result of the $^1J(^{31}P,^{109}Ag)$ and $^1J(^{31}P,^{107}Ag)$ couplings. Therefore, somewhat surprisingly, no $J(P,P)$ couplings are observed, in contrast to the situation with $[Ag\{7,8\text{-}(PPh_2)_2\text{-}7,8\text{-}C_2B_9H_{10}\}(PPh_3)]$, for which all possible cross-couplings are observed. It is noteworthy that the two resonances at $\delta = 43.50$ and 42.81 ppm, although very similar, indicate that the two phosphorus nuclei in $\mathbf{2}^-$ are nonequivalent. The spectrum is shown in Figure 8. This

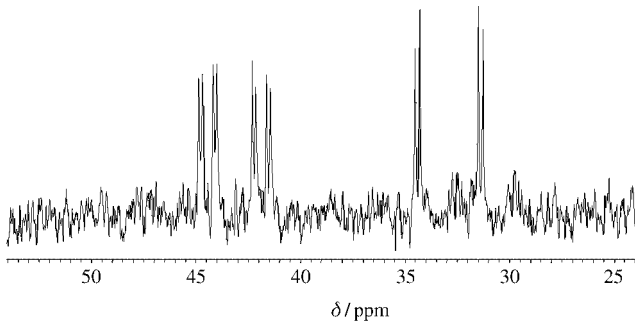

Figure 8. $^{31}P\{^1H\}$ NMR spectrum of **3** recorded in $[D_6]$acetone at −60 °C.

unique behaviour prompted us to synthesize **5**. Once again, the $^{31}P\{^1H\}$ NMR spectrum of **5** was more readily acquired at −60 °C; it features a unique resonance at $\delta = 46.01$ ppm consisting of two doublets due to the $^1J(^{31}P,^{109}Ag)$ and $^1J(^{31}P,^{107}Ag)$ couplings.

The chemical shifts of the chelating phosphorus atoms when Ag is coordinated to $\mathbf{2}^-$, both in **3** and in **5**, are very similar, which is indicative of similar environments in both complexes, although in **3** they are nonequivalent. The only explanation in the case of **3** is that there is not trigonal coordination about Ag, which implies the existence of an extra ancillary ligand, presumably the acetone. The presence of this fourth coordinating ligand would render the molecule asymmetric, and hence the two phosphorus atoms would no longer be equivalent. Moreover, this tetrahedral environment could also account for the fact that no phosphorus cross-couplings are observed in the ^{31}P NMR spectrum. The ambiguity of the situation prompted us to grow crystals to definitively determine the chelating behaviour of $\mathbf{2}^-$.

Crystal structures of 3·OCMe$_2$, 4, and 5: Single crystals of **3**·$OCMe_2$ suitable for X-ray structure analysis were obtained after several days at 22 °C from a solution of **3** in EtOH/acetone. Single crystals of **4** and **5** were similarly obtained from solutions in acetone. Drawings of the three complexes are shown in Figure 9, Figure 10, and Figure 11. Their crystallographic data and structural refinement details are collected in Table 1. Table 3, Table 4, and Table 5 contain selected bond lengths and angles.

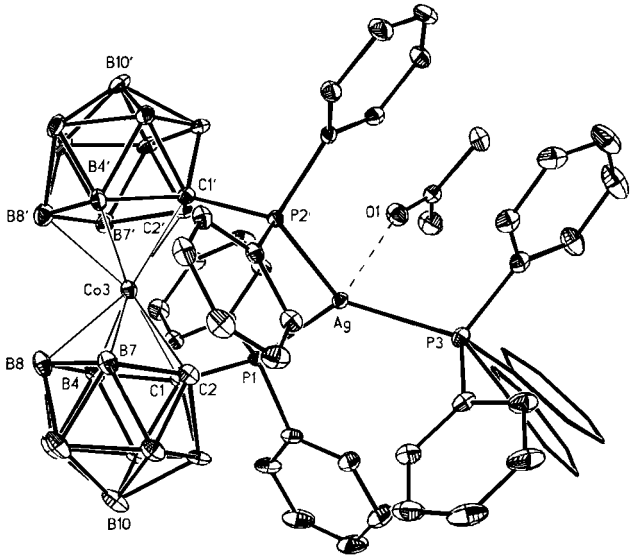

Figure 9. Drawing of [**3**·$OCMe_2$] with 20% thermal displacement ellipsoids. Only skeletons of the two orientations of the disordered phenyl group are shown.

The metal in **3**·$OCMe_2$ and **5** can be viewed as being tetrahedrally coordinated, with one long and three short contacts. The fourth bond in **5** is due to an Ag–H12′ contact of 2.17 Å (equivalent position $-1/2+x$, $3/2-y$, $-1/2+z$), and in **3**·$OCMe_2$ it is due to an Ag···O($OCMe_2$) contact of 2.906(3) Å. Two of the short contacts are due to the two P atoms from $\mathbf{2}^-$, and the third is due to PPh_3 in **3**·$OCMe_2$ and to acetone in **5**. The Ag–H12′[a] and H12′–Ag[b] contacts (equivalent position $1/2+x$, $3/2-y$, $1/2+z$) in **3**·$OCMe_2$ assemble the molecules so as to form a one-dimensional chain. In **4**, Au is tricoordinated to three P atoms, two being provided by $\mathbf{2}^-$ and the third by PPh_3. The trigonal coordina-

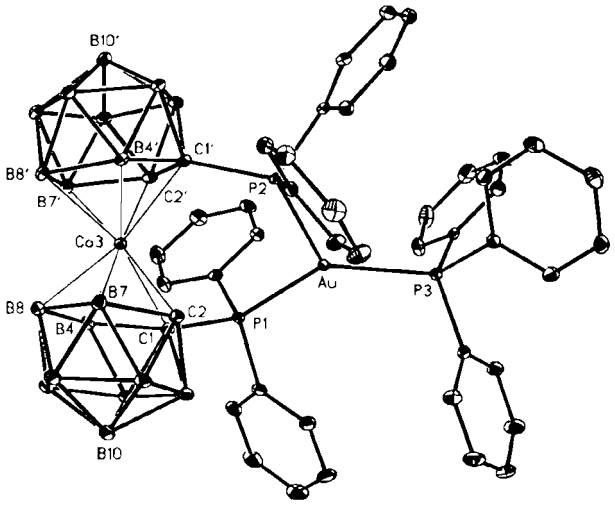

Figure 10. Drawing of **4** with 20% thermal displacement ellipsoids.

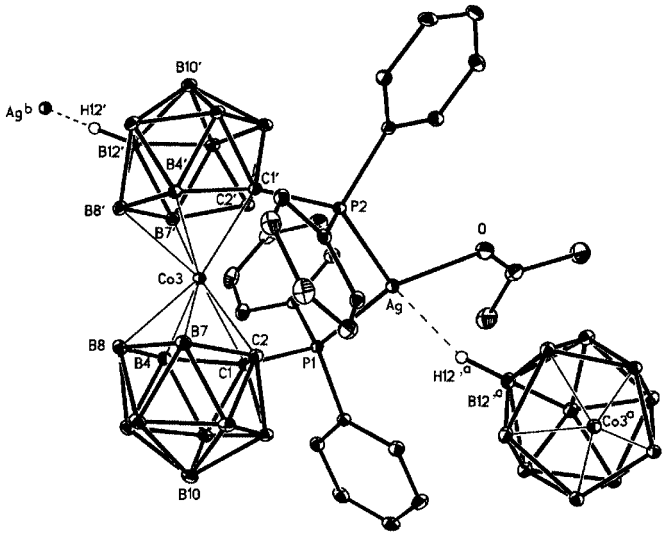

Figure 11. Drawing of **5** (20% thermal displacement ellipsoids) showing how the molecules are connected to neighbouring molecules to form a one-dimensional chain. Intermolecular interactions are drawn with dashes. Hydrogen atoms, with the exception of H12′, have been omitted for clarity. Equivalent positions: [a] $-1/2+x$, $3/2-y$, $-1/2+z$; [b] $1/2+x$, $3/2-y$, $1/2+z$.

Table 3. Selected interatomic distances [Å] and angles [°] for **3**·$OCMe_2$.

Ag–P1	2.5507(9)	Ag–P2	2.5470(10)	Ag–P3	2.4713(10)
Ag–O1	2.906(3)	Co3–C1	2.156(4)	Co3–C2	2.113(4)
Co3–B8	2.153(5)	Co3–C1′	2.158(3)	Co3–C2′	2.096(4)
Co3–B8′	2.158(5)	P1–C1	1.878(4)	P2–C1′	1.878(4)
C1–C2	1.634(5)	C1′–C2′	1.626(5)	P2-Ag-P1	111.21(3)
P3-Ag-P1	129.99(3)	P3-Ag-P2	114.09(3)	C1′-Co3-C1	123.05(14)
C1-P1-Ag	103.79(11)	C1′-P2-Ag	108.87(11)	P1-C1-Co3	112.97(17)
C2-C1-P1	115.1(2)	B4-C1-P1	131.3(3)	P2-C1′-Co3	111.77(17)
C2′-C1′-P2	114.9(2)	B4′-C1′-P2	129.9(3)	B10-Co3-B10′	173.71(11)

tion of Au is further proven by the fact that the Au is displaced by only 0.0648(5) Å from the plane defined by the three P atoms. Likewise, the tetrahedral nature of Ag, both

Table 4. Selected interatomic distances [Å] and angles [°] for **4**.

Au–P1	2.3662(8)	Au–P2	2.4076(8)	Au–P3	2.3467(8)
Co3–C1	2.187(3)	Co3–C2	2.073(3)	Co3–B8	2.138(4)
Co3–C1′	2.163(3)	Co3–C2′	2.060(3)	Co3–B8′	2.154(4)
P1–C1	1.874(3)	P2–C1′	1.878(3)	C1–C2	1.662(4)
C1′–C2′	1.653(4)	P2-Au-P1	107.00(3)	P3-Au-P1	133.08(3)
P3-Au-P2	119.69(3)	C1′-Co3-C1	115.85(11)		
P1-C1-Co3	117.10(15)	C2-C1-P1	118.6(2)		
B4-C1-P1	128.8(2)	P2-C1′-Co3	114.63(15)	C2′-C1′-P2	122.0(2)
B4′-C1′-P2	124.5(2)	B10-Co3-B10′	171.13(8)		

Table 5. Selected interatomic distances [Å] and angles [°] for **5**.

Ag–O	2.3895(17)	Ag–P1	2.4894(6)	Ag–P2	2.4933(6)
Ag–H12′[a]	2.17	Co3–C1	2.153(2)	Co3–C2	2.095(2)
Co3–B8	2.153(3)	Co3–C1′	2.172(2)	Co3–C2′	2.103(2)
Co3–B8′	2.150(3)	P1–C1	1.882(2)	P2–C1′	1.880(2)
C1–C2	1.631(3)	C1′–C2′	1.622(3)	O-Ag-P1	114.68(5)
O-Ag-P2	118.65(5)	P1-Ag-P2	114.746(19)	C1′-Co3-C1	122.51(8)
C1-P1-Ag	104.47(7)	C1′-P2-Ag	107.19(7)	P1-C1-Co3	113.96(11)
C2-C1-P1	114.01(14)	B5-C1-P1	118.40(14)	B4-C1-P1	132.75(17)
B6-C1-P1	105.05(14)	C37-O-Ag	134.76(18)		
P2-C1′-Co3	112.52(11)	B10-Co3-B10′	174.16(5)		

[a] Refers to equivalent position $-1/2+x$, $3/2-y$, $-1/2+z$.

in **3**·$OCMe_2$ and **5**, is proven by the displacement of the Ag atom from the plane defined by the three closest atoms; in **3**·$OCMe_2$ these are three P atoms (displacement of Ag from the plane = 0.3147(7) Å), while in **5** these are the two P atoms and the O atom of the coordinated acetone (displacement of Ag from the plane = 0.4960(8) Å).

The three crystal structures clearly demonstrate the chelating ability of the two phosphorus atoms in $\mathbf{2}^-$. The phosphorus atoms are well separated in [NMe_4]-**2**, as shown by the torsion angle C1-*c*-*c*′-C1′ ($\varphi = -102.3°$), where *c* and *c*′ are the centroids of the pentagonal C_2B_3 faces, but the angle φ is smaller in the complexes, being −77.6°, −54.4°, and −76.4° for **3**·$OCMe_2$, **4**, and **5**, respectively. Figure 12 shows top views of $\mathbf{2}^-$, **3**·$OCMe_2$, **4**, and **5**, focusing on the influence of the metal in dictating the cobaltabisdicarbollide rotamer produced. Interestingly, **4** and **5**, although both having trigonal metal coordination, display a large difference in φ. On the contrary, **3**·$OCMe_2$ and **5**, both of which are Ag complexes, display almost identical φ values despite having the metals in distinctly different immediate environments. This implies that the covalent radius of the metal is the prevailing factor in determining the degree of rotation of the ligand. The longer the M–P bond the larger φ becomes. In this regard, M–P1 and M–P2 distances diminish in the sequence **3**·$OCMe_2$ > **5** > **4**, which mirrors the trend observed for φ. The P1···P2 distances in the coordinated compounds of $\mathbf{2}^-$ are 4.2063(13) Å in **3**·$OCMe_2$, 4.1964(8) Å in **5**, and 3.8374(12) Å in **4**.

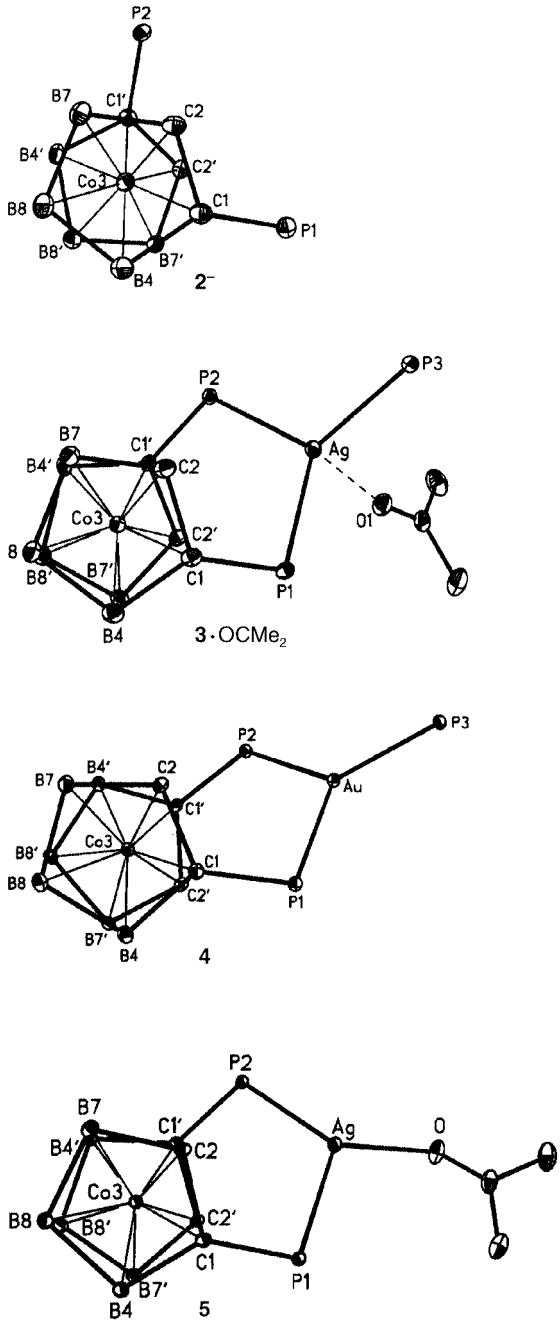

Figure 12. Simplified top views of $\mathbf{2}^-$, $\mathbf{3}\cdot OCMe_2$, **4**, and **5**, focusing on the influence of the metal in dictating the cobaltabisdicarbollide rotamer produced.

With catalytically important elements (Rh and Pd): We also investigated the reaction of $[NMe_4]$-**2** with $[\{Rh(\mu\text{-}Cl)(cod)\}_2]$. Complex $[NMe_4][Rh(\mathbf{2})_2]$ (**6**) was obtained after stirring a mixture of the starting materials in a 4:1 ratio in dichloromethane at room temperature overnight. Complex **6** was isolated in 85% yield as a brown powdery solid, which was found to be partially soluble in acetone. The various resonances in the $^{11}B\{^1H\}$ NMR spectrum overlap greatly, precluding the discernment of a definitive pattern. The resonances are observed in the range $\delta = +7.5$ to -19.5 ppm. The $^{31}P\{^1H\}$ NMR spectrum shows a doublet at $\delta = 85.16$ ppm with $^1J(P,^{103}Rh) = 205$ Hz, in agreement with a structure in which the ligand symmetry has been preserved in the complex, suggesting that the Rh is in a square-planar environment. The strong chelating affinity of P towards Rh was checked by allowing $[NMe_4]$-**2** to react with $[RhCl(PPh_3)_3]$ in refluxing ethanol for 1 h. The resulting complex was again **6**, and was obtained in 87% yield. The stability of **6** in acetone solution was proven by $^{11}B\{^1H\}$ and $^{31}P\{^1H\}$ NMR spectroscopy. No noticeable changes were observed in the spectra, even after several months.

Reaction of $[NMe_4]$-**2** with $[PdCl_2(PPh_3)_2]$ in refluxing ethanol for 1 h yielded a brown complex with the stoichiometry $[PdCl(\mathbf{2})(PPh_3)]$ (**7**). Complex **7** proved to be sparingly soluble in acetone. Its $^{31}P\{^1H\}$ NMR spectrum shows three sets of double doublet resonances at $\delta = 60.39$, 54.02, and 30.37 ppm at $-60\,^\circ C$, indicating non-equivalence of the two binding phosphorus atoms in $\mathbf{2}^-$. The resonance at $\delta = 60.39$ ppm corresponds to the PPh_2 unit *trans* to PPh_3 and appears as a doublet of doublets with the coupling constants $^2J(P_{PPh_{2(trans)}},P_{PPh_3}) = 238$ Hz and $^2J(P_{PPh_2},P_{PPh_2}) = 70$ Hz. The resonance at $\delta = 54.02$ with the coupling constant $^2J(P_{PPh_2},P_{PPh_2}) = 70$ Hz and that at $\delta = 30.37$ ppm with the coupling constant $^2J(P_{PPh_{2(trans)}},P_{PPh_3}) = 238$ Hz correspond to the PPh_2 group located *cis* to PPh_3 and the ancillary PPh_3 ligand, respectively.

Monitoring the evolution of **7** in acetone by $^{11}B\{^1H\}$ and $^{31}P\{^1H\}$ NMR spectroscopy showed $[PdCl(\mathbf{2})(OCMe_2)]$ (**8**) to be the major product after four days. Besides **8**, only traces the unconverted **7** together with some minor unidentified phosphorus-containing products were detected. The $^{31}P\{^1H\}$ NMR spectrum of **8** features two doublets at $\delta = 64.48$ and 54.04 ppm with $^2J(P,P) = 72$ Hz.

Discussion

Ligand $\mathbf{2}^-$ displays similarities with both 1,1′-bis(diphenylphosphino)ferrocene (dppf) and 2,2′-bis(diphenylphosphanyl)-1,1′-binaphthyl (BINAP) (see Figure 1). All of them have the potential to adopt various coordination modes, reflecting their ability to match the steric demands of the coordinated metal, through axial rotation about a C–C bond in BINAP or the centroid···metal···centroid axis in dppf or $\mathbf{2}^-$ (Figure 13). There are, however, important differences between these otherwise similar ligands. The most relevant are: i) whereas $\mathbf{2}^-$ is anionic, BINAP and dppf are neutral; ii) whereas $\mathbf{2}^-$ and BINAP are produced in racemic form, and may therefore be separated into their enantiomers, dppf requires the introduction of a stereogenic center to produce a chiral ligand; and iii) dppf and $\mathbf{2}^-$ have an intense orange color, which is very useful in monitoring purification processes. Overall, $\mathbf{2}^-$ is more similar to BINAP. Additionally, the PPh_2 units in BINAP radiate out from the centroids of the aromatic rings and are tilted towards the C–C axis. This is the origin of the atropisomerism. The possible optical isomerism also originates in this way in $\mathbf{2}^-$, although in this case the chirality has its origin in the C_2B_3 coordinating face with its prochiral carbon atoms. These axial ligands can be regarded as hinges (Figure 14), in which the leaves are each movable fragment, for example, the naphthyl moieties in

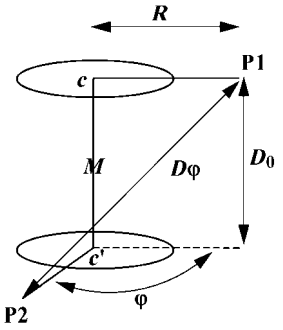

Figure 13. Graphical representation of the terms indicated in Equation (1). Symbols P1 and P2 refer to the metal-coordinating sites of the ligand; in the particular case studied here, they refer to the phosphorus atoms; c and c' represent the points on the hinge axis having R as the minimum distance to P1 and P2; they could represent the centroids in ferrocene derivatives, but not exactly the centroids of the C_2B_3 coordinating faces as in the latter case the C–P bond is tilted towards the metal. M represents the center of the system when $\varphi = 180°$.

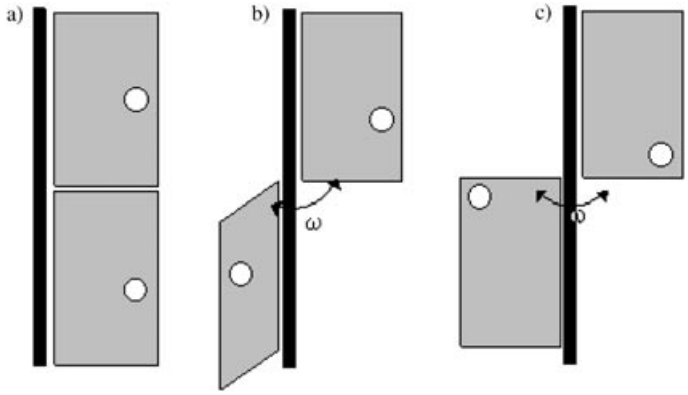

Figure 14. Hole–hole distance preservation by altering D_0 and φ.

BINAP and the dicarbollide moieties in $\mathbf{2}^-$. This representation helps to visualize the great differences between these systems. If the P···Ag···P coordination motif is taken as a reference, it is found that the P···P distance in most diphosphine Ag complexes is practically constant, ranging only from 3.8 to 4.0 Å.[16] Therefore, Ag demands that the two P atoms are geometrically separated by this value. Refering to the hinge shown in Figure 14, one may note that the distance between the holes (PR_2) is maintained constant in a)–c). This has been achieved by varying the distance between the holes in the initial (D_0) position shown in Figure 14a and swinging one of the leaves through the appropriate φ value. Therefore, with the hinge ligands BINAP, dppf, and $\mathbf{2}^-$, practically any required P···P distance can be attained. In Figure 14, hinge situation a) would be representative of dppf, situation b) of $\mathbf{2}^-$, and situation c) of BINAP. Therefore, the plane defined by the "P_2M" moiety will be more aligned with the hinge axis in dppf complexes than in those of BINAP, in the case of which the "P_2M" plane will be practically orthogonal to the axis. An intermediate situation, although closer to that with BINAP, would be that with $\mathbf{2}^-$. All this can be intuitively visualized just by looking at the representations of BINAP, dppf, and $\mathbf{2}^-$ in Figure 1, and estimating the D_0 values, D_0 being the minimum P···P distance that would be achieved when the two phosphorus atoms are in an eclipsed disposition. One would expect that D_0(dppf) > $D_0(\mathbf{2}^-)$ > D_0(BINAP).

It is possible and interesting to assign a quantitative value by which a hinge ligand may be defined. A good indication is provided by the minimum possible P···P distance (D_0). As this hypothetical situation of the two phosphorus atoms being eclipsed is virtually impossible to obtain, and to account for the metal influence, we have developed Equation (1) to determine the D_0 value. Figure 13 displays a graphical representation of the ligand disposition. The D_0 value should be taken with caution as it depends on the metal, the coordination, and other factors, but it gives an indication of the ligand characteristics.

$$D_\varphi^2 = D_0^2 + 4R^2\cos^2(90-\frac{\varphi}{2}) \quad (1)$$

In Equation (1), D_φ = P···P distance at the torsional angle φ; D_0 = P···P distance at the eclipsed position (φ = 0); R = distance of P from the hinge axis; and φ = torsional angle from the eclipsed position. Calculations based on Equation (1) have been performed on data available from crystal structures[17] and those reported in this paper. The computed values average 3.8 Å, 1.1 Å, and 0 Å for dppf, $\mathbf{2}^-$, and BINAP, respectively, which are in perfect agreement with those intuitively deduced above. These three values indicate that dppf will have to swing only very little, through a small φ value, to fit a 4 Å (P···P) demand, for instance. To fit this value, ligand $\mathbf{2}^-$ will have to turn through a larger angle φ, while with BINAP the P···M···P plane will be orthogonal to the hinge axis. The result, therefore, is very different geometrical forms with very similar ligands.

Conclusions

We have described the synthesis of the ligand [1,1′-$(PPh_2)_2$-3,3′-Co(1,2-$C_2B_9H_{10})_2]^-$, $\mathbf{2}^-$, from [3,3′-Co(1,2-$C_2B_9H_{11})_2]^-$ in a one-pot reaction in very good yield and with an easy isolation process. Its two dicarbollide halves swing about an axis in much the same way as the coordinating subunits in BINAP (2,2′-bis(diphenylphosphanyl)-1,1′-binaphthyl) or ferrocenyl phosphine derivatives. We consider these ligands to function as hinges, with the important property of being adjustable to any metal distance demand. Although the [3,3′-Co(1,2-$C_2B_9H_{11})_2]^-$, 1,1′-binaphthyl, and ferrocene backbones show similar torsional behavior, their diphosphino derivatives meet the requirements of metal ions very differently. This is due to the spatial origin and disposition of the PR_2 units. The two PR_2 units in the eclipsed disposition are more separated in the case of the ferrocene backbone than in the cobaltabisdicarbollide system, and, in the latter, more than in the binaphthyl derivatives. Therefore, the "P_2M" plane generated will have a very different relative orientation with respect to the hinge axis. Furthermore, the diphosphine cobaltabisdicarbollide derivative brings the novelty of being an intrinsically coloured, negatively charg-

ed ligand, which apports interesting new possibilities for enhanced coordination and for optional metal site vacancies that otherwise would be fulfilled by a possible anionic monodentate ligand. Ligand $\mathbf{2}^-$ should be separable into its enantiomers and therefore offers the possibility to study the use of intrinsically anionic, enantiomerically pure diphosphine ligands in catalysis. Finally, the ease of synthesis of $\mathbf{2}^-$ opens the possibility of using carborane derivatives as real alternatives to conventional organic ligands.

Experimental Section

General considerations: Elemental analyses were performed using a Carlo Erba EA 1108 microanalyzer. IR spectra were recorded from samples in KBr pellets on a Shimadzu FTIR-8300 spectrophotometer. Mass spectra were recorded in the negative ion mode using a Bruker Biflex MALDI-TOF mass spectrometer [N_2 laser; λ_{exc} = 337 nm (0.5 ns pulses); voltage ion source 20.00 kV (Uis1) and 17.50 kV (Uis2)]. ^{1}H and ^{1}H{^{11}B} NMR (300.13 MHz), ^{13}C{^{1}H} NMR (75.47 MHz), ^{31}P{^{1}H} NMR (121.5 MHz) and ^{11}B and ^{11}B{^{1}H} NMR (96.29 MHz) spectra were recorded on a Bruker ARX 300 instrument equipped with the appropriate decoupling accessories. All NMR spectra were recorded from samples in [D_6]acetone solution. Chemical shift values for the ^{11}B and ^{11}B{^{1}H} NMR spectra were referenced to external $BF_3{\cdot}OEt_2$, ^{31}P{^{1}H} NMR spectra were referenced to external 85% H3PO4 (minus values upfield), and those for the ^{1}H, ^{1}H{^{11}B}, and ^{13}C{^{1}H} NMR spectra were referenced to $SiMe_4$. Chemical shifts are reported in units of parts per million downfield from the reference, and all coupling constants are reported in hertz.

All manipulations were carried out under a dry dinitrogen atmosphere by standard Schlenk techniques. 1,2-Dimethoxyethane (DME) was distilled from sodium benzophenone prior to use. Ethanol and dichloromethane were dried over molecular sieves and deoxygenated prior to use. The Cs-**1** was supplied by Katchem Ltd. (Prague) and was used as received. Reagents were obtained commercially and used as purchased. $[AgClPPh_3]$,[18] $[AuClPPh_3]$,[19] $[\{Rh(\mu\text{-}Cl)(cod)\}_2]$,[20] $[RhCl(PPh_3)_3]$,[21] and $[PdCl_2(PPh_3)_2]$[22] were synthesized according to literature procedures.

Synthesis of [Li(dme)$_2$][1,1′-(PPh$_2$)$_2$-3,3′-Co(1,2-C$_2$B$_9$H$_{10}$)$_2$] ([Li(dme)$_2$]-2): Under an inert atmosphere, *n*-butyllithium (1.6 M in hexanes, 3.4 mL, 5.48 mmol) was added dropwise to a stirred solution of Cs[3,3′-Co(1,2-$C_2B_9H_{11}$)$_2$] (1.25 g, 2.74 mmol) in anhydrous 1,2-dimethoxyethane (120 mL) at −40 °C. The resulting purple solution was stirred for 30 min at low temperature. Then, chlorodiphenylphosphine (1.0 mL, 5.48 mmol) was added, causing a rapid color change to red and the precipitation of a red solid. After the mixture had been stirred for 1 h at room temperature, the solid was collected by filtration, washed with water and petroleum ether, and finally dried in vacuo. Yield: 2.3 g (96%); IR: $\tilde{\nu}$ = 3049 (C_c–H), 2927, 2898 (C_{aryl}–H), 2548 (B–H), 1433, 1084, 746, 698, 499 cm^{-1}; ^{1}H NMR: δ = 7.76, 7.54, 7.46, 7.31 (m, 20H; Ph), 4.37 (brs, 2H; C_c–H), 3.46 (s, 8H; CH_2 of DME), 3.28 (s, 12H; CH_3 of DME), 4.14–1.25 ppm (brm, 18H; B–H); ^{1}H{^{11}B} NMR: δ = 7.76, 7.54, 7.46, 7.31 (m, 20H; Ph), 4.37 (brs, 2H; C_c–H), 3.46 (s, 8H; CH_2 of DME), 4.14 (brs, 2H; B–H), 3.28 (s, 12H; CH_3 of DME), 3.21 (brs, 2H; B–H), 2.89 (brs, 4H; B–H), 2.21 (brs, 2H; B–H), 1.92 (brs, 4H; B–H), 1.47 (brs, 2H; B–H), 1.25 ppm (brs, 2H; B–H); ^{13}C{^{1}H} NMR: δ = 139.05 (d, ^1J(P,C) = 22 Hz; P–C_{ipso}), 137.05 (d, ^1J(P,C) = 17 Hz; P–C_{ipso}), 135.23 (d, ^2J(P,C) = 29 Hz; *o*-C(Ph)), 134.27 (d, ^2J(P,C) = 26 Hz; *o*-C(Ph)), 129.54 (s; *p*-C(Ph)), 128.51 (s; *p*-C(Ph)), 128.18 (d, ^3J(P,C) = 8 Hz; *m*-C(Ph)), 127.31 (d, ^3J(P,C) = 8 Hz; *m*-C(Ph)), 71.64 (s; CH_2 of DME), 61.41 (d, ^1J(P,C) = 81 Hz; P–C_c), 60.22 (dd, ^2J(P,C) = 47 Hz, ^3J(P,C) = 14 Hz; C_c–H), 57.50 ppm (s; CH_3 of DME); ^{11}B NMR: δ = 9.1 (d, ^1J(B,H) = 127 Hz, 2B), 2.3 (d, ^1J(B,H) = 137 Hz, 2B), −3.3 (d, ^1J(B,H) = 106 Hz, 4B), −4.2 (d, ^1J(B,H) = 98 Hz, 4B), −13.7 (d, ^1J(B,H) = 183 Hz, 2B), −15.9 (d, ^1J(B,H) = 163 Hz, 2B), −20.0 ppm (d, ^1J(B,H) = 137 Hz, 2B); ^{31}P{^{1}H} NMR: δ = 23.48 ppm (s; C_c–PPh_2); MALDI-TOF MS: *m*/*z* (%): 691.43 (*M*, 9), 507.33 (*M*−PPh_2, 73), 323.32 (*M*−2PPh_2, 100); elemental analysis calcd (%) for $C_{36}H_{60}B_{18}CoLiO_4P_2$: C 49.18, H 6.88; found: C 48.95, H 7.00.

Synthesis of [Ag{1,1′-(PPh$_2$)$_2$-3,3′-Co(1,2-C$_2$B$_9$H$_{10}$)$_2$}(PPh$_3$)]·OCMe$_2$ (3): $[AgClPPh_3]$ (0.034 g, 0.08 mmol) was added to a suspension of $[NMe_4]$[1,1′-$(PPh_2)_2$-3,3′-Co(1,2-$C_2B_9H_{10})_2$] (0.06 g, 0.08 mmol) in EtOH (10 mL) and the resulting mixture was refluxed for 30 min. The maroon solid formed was then collected by filtration and washed with ethanol and water. Yield: 59 mg (71%); IR: $\tilde{\nu}$ = 3058 (C_c–H), 2557 (B–H), 1359 (C–O), 1436, 1096, 743, 691, 502 cm^{-1}; ^{1}H NMR: δ = 8.30, 7.35, 6.37 (m, 35H; Ph), 4.41–0.88 (brm, 18H; B–H), 4.83 (brs, 2H; C_c–H), 2.09 ppm (s, 6H; CH_3); ^{13}C{^{1}H} NMR: δ = 205.12 (s; CO), 137.55 (s; Ph), 135.82 (s; Ph), 133.69 (d, J(P,C) = 17 Hz; Ph), 130.01 (s; Ph), 128.94 (d, J(P,C) = 8 Hz; Ph), 127.95 (s; Ph), 126.35 (s; Ph), 61.14 (s; C_c), 28.99 ppm (s, CH_3); ^{11}B NMR: δ = 9.9 (d, ^1J(B,H) = 105 Hz, 2B), 3.2 (d, ^1J(B,H) = 107 Hz, 2B), −3.1 (d, ^1J(B,H) = 110 Hz, 8B), −13.1 (d, ^1J(B,H) = 175 Hz, 2B), −15.0 (d, ^1J(B,H) = 145 Hz, 2B), −19.1 ppm (d, 2B); ^{31}P{^{1}H} NMR (−60 °C): δ = 43.50 (2d, ^1J(^{109}Ag,P) = 330 Hz, ^1J(^{107}Ag,P) = 286 Hz, 1P; PPh_2), 42.81 (2d, ^1J(^{109}Ag,P) = 330 Hz, ^1J(^{107}Ag,P) = 286 Hz, 1P; PPh_2), 32.89 ppm (2d, ^1J(^{109}Ag,P) = 392 Hz, ^1J(^{107}Ag,P) = 366 Hz, 1P; PPh_3); elemental analysis calcd (%) for $C_{49}H_{61}AgB_{18}CoOP_3$: C 52.53, H 5.49; found: C 52.79, H 5.34.

Synthesis of [Au{1,1′-(PPh$_2$)$_2$-3,3′-Co(1,2-C$_2$B$_9$H$_{10}$)$_2$}(PPh$_3$)] (4): $[AuClPPh_3]$ (0.034 g, 0.07 mmol) was added to a solution of Cs[1,1′-$(PPh_2)_2$-3,3′-Co(1,2-$C_2B_9H_{10})_2$] (0.06 g, 0.07 mmol) in EtOH (10 mL). The complex, a red solid, was collected by filtration after refluxing for 30 min. Yield: 89 mg (98%); IR: $\tilde{\nu}$ = 3069 (C_c–H), 2573, 2550 (B–H), 1435, 1094, 746, 692 cm^{-1}; ^{1}H NMR: δ = 7.83, 7.61, 7.44, 7.36 (m, 35H; Ph), 4.42 (brs, 2H; C_c–H), 4.17–0.89 ppm (brm, 18H; B–H); ^{1}H{^{11}B} NMR: δ = 7.83, 7.61, 7.44, 7.36 (m, 35H; Ph), 4.42 (brs, 2H; C_c–H), 4.17 (brs, 2H; B–H), 3.30 (brs, 2H; B–H), 2.81 (brs, 4H; B–H), 2.19 (brs, 2H; B–H), 1.93 (brs, 4H; B–H), 1.31 (brs, 2H; B–H), 0.89 ppm (brs, 2H; B–H); ^{13}C{^{1}H} NMR: δ = 135.90 (d, J(P,C) = 26 Hz, Ph), 134.79 (d, J(P,C) = 25 Hz, Ph), 134.02 (d, J(P,C) = 14 Hz, Ph), 132.07 (s, Ph), 130.16 (s, Ph), 129.48 (d, J(P,C) = 11 Hz, Ph), 128.20 (d, J(P,C) = 34 Hz, Ph), 60.77 ppm (s, C_c–H); ^{11}B NMR: δ = 10.0 (d, ^1J(B,H) = 116 Hz, 2B), 3.0 (d, ^1J(B,H) = 152 Hz, 2B), −3.0 (d, ^1J(B,H) = 135 Hz, 4B), −5.1 (d, ^1J(B,H) = 174 Hz, 4B), −13.1 (d, ^1J(B,H) = 147 Hz, 2B), −15.4 (d, ^1J(B,H) = 144 Hz, 2B), −19.4 ppm (d, ^1J(B,H) = 152 Hz, 2B); ^{31}P{^{1}H} NMR (−60 °C): δ = 73.61 (d, $^2J(P_{PPh_2},P_{PPh_3})$ = 146 Hz, 2P; PPh_2), 45.06 (t, $^2J(P_{PPh_2},P_{PPh_3})$ = 146 Hz, 1P; PPh_3); elemental analysis calcd (%) for $C_{46}H_{55}AuB_{18}CoP_3$: C 47.99, H 4.81; found: C 47.95, H 4.63.

Synthesis of [Ag{1,1′-(PPh$_2$)$_2$-3,3′-Co(1,2-C$_2$B$_9$H$_{10}$)$_2$}(OCMe$_2$)] (5): A solution of $[AgClO_4]$ (0.016 g, 0.08 mmol) in acetone (1 mL) was added to a solution of $[NMe_4]$[3,3′-Co(1-PPh_2-1,2-$C_2B_9H_{10})_2$] (0.06 g, 0.08 mmol) in a mixture of EtOH (10 mL) and acetone (3 mL). The mixture was stirred at room temperature overnight. Concentration of the mixture led to the precipitation of a pink solid. This was collected by filtration, washed with water and petroleum ether, and dried in vacuo. Yield: 59.2 mg (88%); IR: $\tilde{\nu}$ = 3058 (C_c–H), 2563, 2509 (B–H), 1310 (C–O), 1436, 1088, 741, 687 cm^{-1}; ^{1}H NMR: δ = 8.21 (brs, 5H; Ph), 8.09 (brs, 5H; Ph), 7.53, 7.45 (m, 10H; Ph), 4.73 (brs, 2H; C_c–H), 4.47–0.88 (brm, 18H; B–H), 2.09 ppm (s, 6H; CH_3); ^{13}C{^{1}H} NMR: δ = 205.17 (s; CO), 137.23 (s; Ph), 135.38 (s; Ph), 132.46 (s; Ph), 131.81 (s; Ph), 131.24 (s; Ph), 128.83 (s; Ph), 128.06 (s; Ph), 62.26 (s; C_c–H), 28.90 ppm (s; CH_3); ^{11}B NMR: δ = 12.7 (brs, 2B), 3.8 (d, ^1J(B,H) = 132 Hz, 2B), −0.2 (d, ^1J(B,H) = 134 Hz, 2B), −4.0 (d, ^1J(B,H) = 118 Hz, 4B), −7.0 (brs, 2B), −12.7 (brs, 2B), −15.2 (brs, 2B), −20.4 ppm (d, ^1J(B,H) = 141 Hz, 2B); ^{31}P{^{1}H} NMR: δ = 46.01 (2d, ^1J(^{109}Ag,P) = 463 Hz, ^1J(^{107}Ag,P) = 403 Hz, 2P; PPh_2); elemental analysis calcd (%) for $C_{31}H_{46}AgB_{18}CoOP_2$: C 43.39, H 5.40; found: C 43.20, H 5.31.

Synthesis of [NMe$_4$][Rh{1,1′-(PPh$_2$)$_2$–3,3′-Co(1,2-C$_2$B$_9$H$_{10}$)$_2$}$_2$] (6): a) Starting from [{Rh(μ-Cl)(cod)}$_2$]: [{Rh(μ-Cl)(cod)}$_2$] (0.032 g, 0.065 mmol) was added to a solution of $[NMe_4]$-**2** (0.2 g, 0.26 mmol) in deoxygenated dichloromethane (10 mL) and the solution was stirred at room temperature overnight. A brown solid that separated was collected by filtration and washed with ethanol (10 mL) and water to give **6**. Yield: 174 mg (85%).

b) Starting from $[RhCl(PPh_3)_3]$: $[RhCl(PPh_3)_3]$ (0.120 g, 0.13 mmol) was added to a solution of $[NMe_4]$-**2** (0.2 g, 0.26 mmol) in deoxygenated ethanol (10 mL) and the mixture was refluxed for 1 h. A brown solid that sep-

arated was collected by filtration and washed with ethanol (10 mL) and water to give **6**. Yield: 172 mg (87%); IR: $\tilde{\nu}$ = 3059 (C_c–H), 2558 (B–H), 1481, 1435, 1080, 943, 745, 694 cm^{-1}; ^1H NMR: δ = 8.53, 8.05–7.01 (m, 40H; Ph), 4.28 (brs, 4H; C_c–H), 3.40 ppm (s, 12H; NMe_4); ^{11}B NMR: δ = 7.5, 3.6, −2.8, −6.5, −13.6, −19.5 ppm (36B); $^{31}P\{^1H\}$ NMR: δ = 85.16 (d, $^1J(^{31}P,^{103}Rh)$ = 205 Hz; PPh_2); elemental analysis calcd (%) for $C_{60}H_{92}B_{36}Co_2NP_4Rh$: C 46.16, H 5.94, N 0.90; found: C 45.97, H 5.72, N 1.10.

Synthesis of [PdCl{3,3′-Co(1-PPh_2-1,2-$C_2B_9H_{10}$)$_2$}(PPh_3)] (7): $[PdCl_2(PPh_3)_2]$ (0.183 g, 0.26 mmol) was added to a solution of $[NMe_4]$-**2** (0.2 g, 0.26 mmol) in deoxygenated ethanol (10 mL) and the mixture was refluxed for 1 h. A brown solid that separated was collected by filtration and washed with ethanol (10 mL) and water to give **7**. Yield: 270 mg (94%); IR: $\tilde{\nu}$ = 3060 (C_c–H), 2563 (B–H), 1435, 1099, 745, 692 cm^{-1}; ^1H NMR: δ = 8.25–7.39 (m, 35H; Ph), 4.51 (brs, 1H; C_c–H), 4.31 ppm (brs, 1H; C_c–H); ^{11}B NMR: δ = 9.7, 5.7, −0.05, −2.1, −3.8, −13.1, −20.9 ppm (18B); $^{31}P\{^1H\}$ NMR: δ = 60.39 (dd, $^2J(P_{PPh_{2(trans)}},PPh_3)$ = 238 Hz, $^2J(P_{PPh_2},P_{PPh_2})$ = 70 Hz, 1P; PPh_2 *trans* to PPh_3), 54.02 (d, $^2J(P_{PPh_2})$,P_{PPh_2})) = 70 Hz, 1P; PPh_2 *cis* to PPh_3), 30.37 ppm (d, $^2J(P_{PPh_{3(trans)}},P_{PPh_3})$) = 238 Hz, 1P; PPh_3); elemental analysis calcd (%) for $C_{46}H_{55}B_{36}ClCoP_3Pd$: C 50.40, H 5.06; found: C 50.76, H 4.93.

X-ray crystallography: Single-crystal X-ray data for $[NMe_4]$-**2** were collected at ambient temperature on a Rigaku AFC5S diffractometer, while the collections for **3**·$OCMe_2$, **4**, and **5** were performed at −100°C on an Enraf-Nonius KappaCCD diffractometer using graphite-monochromated $Mo_{K\alpha}$ radiation. A total of 7438, 9571, 8850, and 8990 unique reflections were collected for $[NMe_4]$-**2**, **3**·$OCMe_2$, **4**, and **5**, respectively. The structures were solved by direct methods and refined against F^2 using the SHELXL-97 program.[23] For all structures, the hydrogen atoms were treated as riding atoms using the SHELXL-97 default parameters. For $[NMe_4]$-**2**, all non-hydrogen atoms were refined with anisotropic displacement parameters. For **3**·$OCMe_2$, one of the phenyl groups connected to P3 and the non-coordinated acetone solvent molecule were found to be disordered, both assuming two orientations. The disordered groups were refined as rigid groups and non-hydrogen atoms of these groups were refined with isotropic thermal displacement parameters. The rest of the non-hydrogen atoms were refined with anisotropic displacement parameters. For **4** and **5**, all non-hydrogen atoms were refined with anisotropic displacement parameters.

CCDC-216061–216064 contain the supplementary crystallographic data for this paper. These data can be obtained free of charge via www.ccdc.cam.ac.uk/conts/retrieving.html (or from the Cambridge Crystallographic Data Centre, 12 Union Road, Cambridge CB2 1EZ, U.K.; fax: (+44) 1223-336033; or e-mail: deposit@ccdc.cam.ac.uk).

Acknowledgement

We thank ENRESA for partial support of this research, the MCyT (MAT01–1575), and the Generalitat de Catalunya (2001/SGR/00337).

[1] a) B. Cornils, W. A. Herrmann, *Applied Homogeneous Catalysis with Organometallic Complexes*, A Comprehensive Handbook 2, vols. 1 & 2, Wiley-VCH, Weinheim, **2002**; b) G. W. Parshall, S. D. Ittel, *Homogeneous Catalysis. The Applications and Chemistry of Catalysis by Soluble Transition Metals Complexes*, 2nd Ed., Wiley Interscience, New York, **1992**; c) A. N. Collins, G. N. Sheldrake, J. Crosby, *Chirality in Industry. The Commercial Manufacture and Application of Optically Active Compounds*, John Wiley and Sons, Chichester, **1992**.

[2] a) W. S. Knowles, M. J. Sabacky, *Chem. Commun.* **1968**, 1445; b) W. S. Knowles, *Angew. Chem.* **2002**, *114*, 2096; *Angew. Chem. Int. Ed.* **2002**, *41*, 1998.

[3] L. Horner, H. Siegel, H. Büthe, *Angew. Chem.* **1968**, *80*, 1034; *Angew. Chem. Int. Ed. Engl.* **1968**, *7*, 942.

[4] T. P. Dang, H. B. Kagan, *J. Chem. Soc. Chem. Commun.* **1971**, 481.

[5] A. Miyashita, A. Yasuda, H. Kakaya, K. Toriumi, T. Ito, T. Souchi, R. Noyori, *J. Am. Chem. Soc.* **1980**, *102*, 7932.

[6] a) R. Noyori, *Acc. Chem. Res.* **1990**, *23*, 345; b) R. Noyori, *Tetrahedron* **1994**, *50*, 4259; c) R. Noyori, *Angew. Chem.* **2002**, *114*, 2108; *Angew. Chem. Int. Ed.* **2002**, *41*, 2008.

[7] a) *Handbook of Enantioselective Catalysis*, (Eds.: H. Brunner, W. Zettlmeier) VCH, New York, **1993**; b) *Comprehensive Asymmetric Catalysis*, (Eds.: E. N. Jacobsen, A. Pfaltz, H. Yamamoto), Springer, New York, **1999**.

[8] a) R. Noyori, H. Takaya, *Acc. Chem. Res.* **1990**, *23*, 345; b) H. Takaya, T. Ohta, R. Noyori, in *Catalytic Asymmetric Synthesis* (Ed.: I. Ojima), VCH, New York, **1993**; c) *Catalytic Asymmetric Synthesis*, (Ed.: I. Ojima) 2nd edition, VCH, New York, **2000**; d) R. Noyori, *Asymmetric Catalysis in Organic Synthesis*, Wiley, New York, **1994**.

[9] a) R. Schmid, M. Cereghetti, B. Heiser, P. Schonholzer, H.-J. Hansen, *Helv. Chim. Acta* **1988**, *71*, 897; b) R. Schmid, J. Foricher, M. Cereghetti, P. Schonhoizer, *Helv. Chim. Acta* **1991**, *74*, 370; c) R. Schmid, E. A. Broger, M. Cereghetti, Y. Crameri, J. Foricehr, M. Lalonde, R. K. Muller, M. Scalone, G. Schoettel, U. Zutter, *Pure Appl. Chem.* **1996**, *68*, 131.

[10] Z. Zhang, H. Qian, J. Longmire, X. Zhang, *J. Org. Chem.* **2000**, *65*, 6223.

[11] a) P. Lustenberger, E. Martinborough, T. M. Denti, F. Diederich, *J. Chem. Soc. Perkin Trans. 2* **1998**, 747; b) T. Harada, M. Takeuchi, M. Hatsuda, S. Ueda, A. Oku, *Tetrahedron: Asymmetry* **1996**, *7*, 2479; c) B. H. Lipshutz, Y.-J. Shin, *Tetrahedron Lett.* **1998**, *39*, 7017.

[12] S. A. Raynor, J. M. Thomas, R. Raja, B. F. G. Johnson, R. G. Bell, M. D. Mantle, *Chem. Commun.* **2000**, 1925.

[13] I. B. Sivaev, V. I. Bregadze, *Collect. Czech. Chem. Commun.* **1999**, *64*, 783.

[14] a) K. T. Wan, M. E. Davis, *J. Catal.* **1994**, *148*, 1; b) Q.-H. Fan, Y.-M. Li, A. S. C. Chan, *Chem. Rev.* **2002**, *102*, 3385.

[15] O. Crespo, C. Gimeno, A. Laguna, *J. Chem. Educ.* **2000**, *77*, 86.

[16] G. Bandoli, A. Dolmella, *Coord. Chem. Rev.* **2000**, *209*, 161.

[17] a) M. C. Gimeno, P. G. Jones, A. Laguna, C. Sarroca, *J. Chem. Soc. Dalton Trans.* **1995**, 1473; b) A. Miyashita, A. Yasuda, H. Takaya, K. Toriumi, T. Ito, T. Souchi, R. Noyori, *J. Am. Chem. Soc.* **1980**, *102*, 7932; c) A. J. Deeming, D. M. Speel, M. Stchedroff, *Organometallics* **1997**, *16*, 6004.

[18] P. H. Davis, R. L. Belford, I. C. Paul, *Inorg. Chem.* **1973**, *12*, 213.

[19] a) M. L. Malvano, *Atti. Rend. Accad. Lincei* **1908**, *17*, 847; b) M. I. Bruce, B. K. Nicholson, O. Bin Shawkataly, *Inorg. Synth.* **1989**, *26*, 324.

[20] D. F. Schriver, *Inorg. Synth.* **1979**, *19*, 218.

[21] J. A. Osborn, G. Wilkinson, *Inorg. Synth.* **1967**, *10*, 67.

[22] J. R. Blackburn, R. Nordberg, F. Stevie, R. G. Albridge, M. M. Jones, *Inorg. Chem.* **1970**, *9*, 2374.

[23] G. M. Sheldrick, SHELXL-97, University of Göttingen, Germany, **1997**.

Received: April 13, 2004
Published online: September 20, 2004

